Microwave Compact Biconical Antenna with Low Diffraction Lobes for UAV Control Systems with Protection from Jamming

Stepan Piltyay and Mykhailo Omelianenko
Radio Engineering Faculty, National Technical University of Ukraine "Igor Sikorsky Kyiv Polytechnic Institute", Kyiv, Ukraine

Corresponding author: Stepan Piltyay (e-mail: crosspolar@ukr.net).

ABSTRACT Results of theoretical investigation, numerical simulation, constructive development and experimental measurements of new compact biconical antenna for UAVs are presented in this article. Peculiarity of designed antenna consists in low diffraction lobes in its radiation pattern. This feature was achieved by using dielectric disc in the center region of antenna's structure between conducting cones. Operating frequencies of antenna in the microwave range ensure protection from electronic jamming systems with quasi-isotropic antennas. Due to high attenuation of radiated electromagnetic waves at microwave frequencies, only directed antennas can create effective jamming of UAV in this band. Such possibility of adverse impact on UAV control system is excluded by low diffraction lobes of applied antenna and a priori unknown operation frequency of wireless control system. Measured results showed that at operating frequency designed antenna with coaxial-to-waveguide transition has VSWR equal to 1.6, maximal value of gain is 6.3 dBi. Measured diffraction lobes of radiation pattern in range of elevation angle −30–+30° from the antenna's axis are less than −20 dBi. Designed compact biconical antennas were successfully used in new UAV control systems for military applications.

INDEX TERMS Biconical antenna, diffraction, microwave antenna, omnidirectional antenna, radiation pattern, side lobes, unmanned aerial vehicle.

I. INTRODUCTION

ANTENNAS with horizontally undirected radiation and reception of signals are commonly used in wireless control systems for terrestrial [1], aerial [2], and marine vehicles [3]. Dynamically developing engineering landscape of systems applying unmanned aerial vehicle (UAV) solutions requires reliable wireless communication for control, data transmission and navigation. One can mention relevant applications including reconnaissance [4], surveillance [5] and management [6] in modern areas of agriculture [7], security systems [8], measurements [9], disasters prediction [10], infrastructure inspection [11], logistics [12], and delivery [13]. In addition to listed civil applications, robust performance of wireless communication system of UAV can have paramount influence on military missions' success [14].

From points of view of convenience and simplicity antennas with omnidirectional radiation pattern [15], [16] are the best choice for communication with vehicles including UAV. Vehicle's mobility leads to variations in on-board antenna's position, direction and inclination angle relative to the base station or an operator's antenna. Under these conditions only antenna with wide angular width of radiation pattern in both E- and H-planes is a suitable solution.

Recently, biconical antenna designs have become effective alternative to simple omnidirectional half-wave dipoles [17], [18], [19]. Principal advantages of biconical antenna include possibilities to provide various required frequency bandwidths from narrow to ultrawide ones. Besides, application of addition polarizer allows biconical antenna to receive or transmit signals carried by electromagnetic waves with different polarizations except of cross-polarization [20], [21], [22]. Polarization transformers in waveguide technology typically include diaphragms [23], [24], posts [25], [26], and their combinations [27]. In contrast to commonly used waveguide polarization converters [28], polarizer of biconical antenna is placed over the whole aperture and contains layers of inclined conducting strips on a substrate from dielectric material [20], [21], [22]. The third feature of biconical antenna is a blockage of radiation in directions upward and downward relative to horizontal plane by conducting cones. This property of biconical antenna makes it a unique candidate for wireless systems of military UAVs with protection from jamming.

Electronic warfare systems for protection from aerial strikes by combat drones transmit electromagnetic interferences by quasi-isotropic antennas of clover [29] or turnstile type [30], [31]. As a result, occurring jamming

represents a serious threat for aerial operation. It can severely disrupt UAV's wireless communication with operator or base station, leading to signal failures or critical loss of flight control.

The application of a biconical antenna on board of UAV automatically provides spatial protection from jamming by conducting surfaces in the structure, making its design an ultimate choice for combat UAVs. In addition, this can be effectively combined with other anti-jamming methods. For example, wide operating frequency band of biconical antenna provides possibility of simultaneous communication in multiple channels, which allows implementing advanced signal processing methods [32], [33] and frequency hopping techniques [34] that would reduce the adverse influence of the jamming interference.

Engineering technique for protection from jamming, which was suggested and developed by the authors, consists in conversion of UAV control signals up to the microwave carrier frequency, communication of an operator and UAV at this frequency, and reverse down frequency conversion by on-board electronic equipment of UAV. This solution makes each combat UAV more expensive in 1.5–2 times, but probability of successful strikes under jamming conditions would sufficiently rise. Technical requirements for developed antenna include compact design, low weight, value of voltage standing wave ratio (VSWR) less than 2 at operating frequency of 22 GHz, moderate gain of antenna within values of 5–8 dBi, and diffraction lobes of radiation pattern in range of elevation angle −30–+30° from the antenna's axis of symmetry less than −14 dBi.

II. STRUCTURE OF BICONICAL ANTENNA WITH LOW DIFFRACTION LOBES OF RADIATION PATTERN

Geometrical model of the developed compact biconical antenna is presented in Fig. 1. Total view of the antenna is shown in Fig. 1 (a), and its axial section is demonstrated in Fig. 1 (b). In addition, Fig. 1 (b) illustrates main elements of antenna's structure, which include two metal conical surfaces (1) and (2), dielectric disc (3), feeding coaxial transmission line (4), and cylindrical dielectric spacer (5). As it is seen in Fig. 1, antenna's diameter and height are equal to 120 mm and 41 mm, respectively.

For the possibility of manufacturing of real antenna design the materials of its elements were chosen at the stage of numerical simulation. Calculations of the designed antenna's matching and radiation characteristics were performed using software CST Microwave Studio.

Metal of conducting conical surfaces and of coaxial line conductors is copper, although it was modeled as perfect electric conductor (PEC). Calculations of electromagnetic characteristics of an antenna with components made from PEC are much faster compared to modeling of metal with losses, and obtained results are practically identical in the microwave frequency range. Two fabricated copper conical surfaces are presented in Fig. 2. One of them contains inner conductor of feeding coaxial transmission line and matching bead. Another conical surface is integrated with outer conductor of the coaxial line.

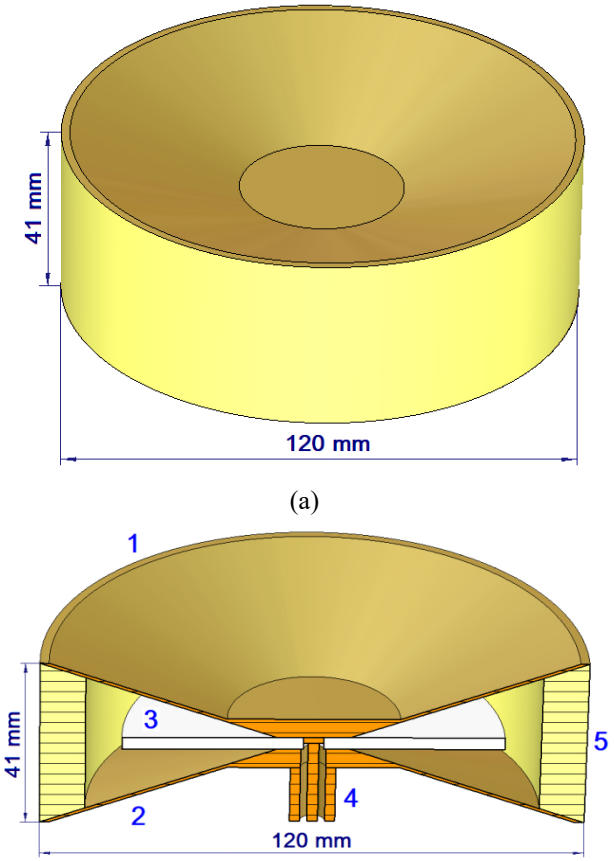

FIGURE 1. Total view (a) and axial section (b) of biconical antenna.

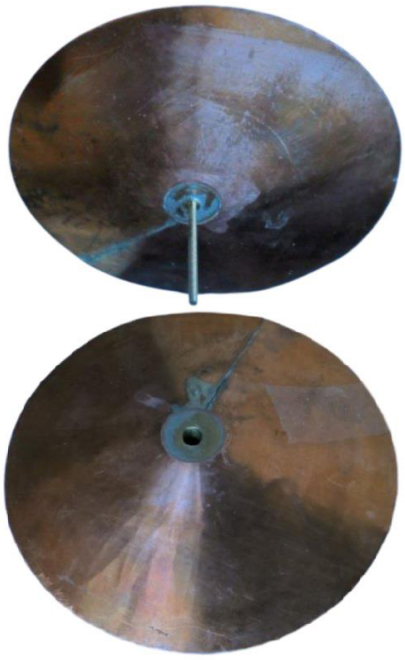

FIGURE 2. Two conical surfaces fabricated from copper.

Teflon was chosen as material of dielectric disc (3) due to its hardness, stability, low losses, and simplicity of mechanical processing. According to results from [35], in numerical simulation process Teflon disc's permittivity was equal to 2.

Dielectric spacer (5) must be transparent for microwave range radiation, possess light weight and protect antenna from adverse weather conditions. Consequently, the most suitable material for spacer fabrication is Polyurethane foam. Based on results from [36], in numerical calculations Polyurethane foam's permittivity was equal to 1.2. Fabricated Teflon disc and Polyurethane foam spacer are demonstrated in Fig. 3.

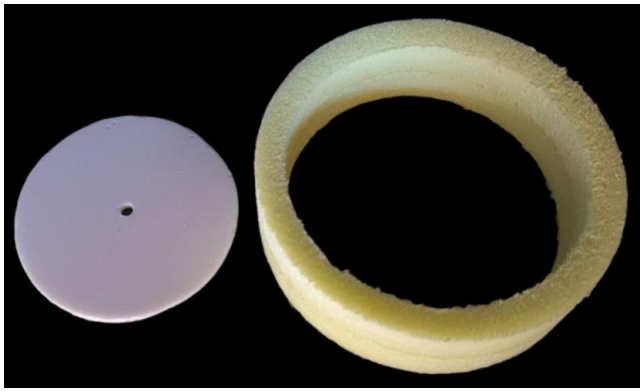

FIGURE 3. Fabricated Teflon disc and Polyurethane foam spacer.

III. NUMERICAL RESULTS OF MATCHING AND RADIATION PERFORMANCE OF ANTENNA WITH LOW DIFFRACTION LOBES

A parametric optimization was carried out to obtain minimal diffraction lobes of antenna's radiation pattern at operating frequency 22 GHz. Construction limitations of optimization included fixed diameter on cones (120 mm), which is determined by UAV platform sizes. To provide rigidity of antenna structure, thickness of Polyurethane foam spacer was fixed at the value of 10 mm.

Three geometrical parameters were altered during the minimization of diffraction lobes. They are biconical antenna's height, Teflon disc height, and disc's diameter, which automatically determined gap between conducting conical surfaces. Obtained optimal sizes (for the operating frequency of 22 GHz) are presented in Table I.

TABLE I. Sizes of Biconical Antenna with Minimal Diffraction Lobes

Size	Numerical value, mm
Diameter of antenna	120
Height of antenna	41
Diameter of Teflon disc	84
Height of Teflon disc	3
Diameter of circular hole in Teflon disc	4.4
Diameter of conducting matching bead	4.4
Height of conducting matching bead	1.5
Gap between conducting cones	3
Thickness of polyurethane foam spacer	10

Fig. 4 presents numerically modeled functions of VSWR versus frequency for developed microwave biconical antenna with sizes listed in Table I. Simulation model was shown before in Fig. 1 and it didn't include coaxial-to-waveguide transition. As it is seen in Fig. 4, theoretical values of VSWR are less than 1.5 in the range of frequencies from 20 to 24 GHz. At the operating frequency of 22 GHz simulated VSWR of antenna without transition is equal to 1.3.

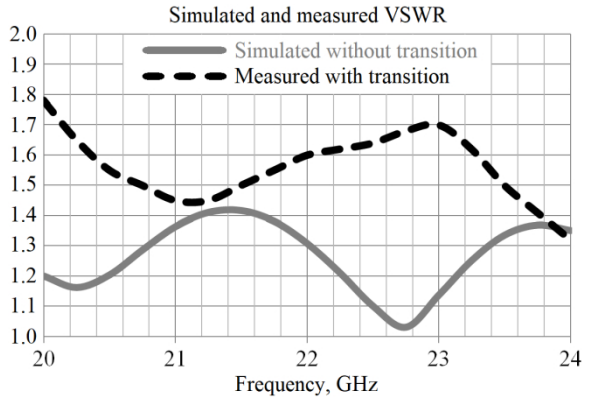

FIGURE 4. Simulated and measured VSWR of biconical antenna.

Calculated E-plane gain radiation pattern (in dBi) of developed antenna at the operating frequency of 22 GHz is shown in Fig. 5. In addition, results for the biconical antenna without a dielectric disc are also presented. Shown in Fig. 5 radiation patterns demonstrate the reduction of diffraction lobes for antenna with suggested dielectric disc for elevation angles from 60 to 90° (identical to elevation angle variation −30–+30° from the antenna's axis of symmetry) by more than 5 dB. Besides, first-order side lobes of radiation pattern (at elevation angle $\theta = \pm 28°$) are absent for the antenna with dielectric disc. Simulated results show that maximal gain of antennas with and without dielectric disc are equal to 6.3 and 6.6 dBi, respectively.

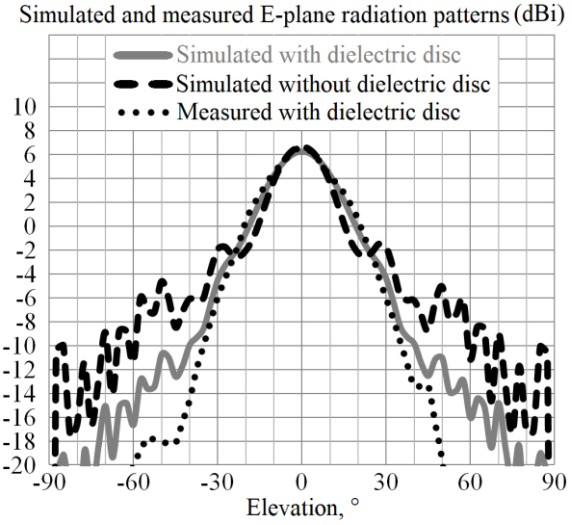

FIGURE 5. Simulated and measured E-plane gain radiation patterns.

IV. THEORETICAL EXPLANATION OF DIFFRACTION LOBES IN RADIATION PATTERN OF BICONICAL ANTENNA

Values of elevation angles θ_n corresponding to maximum of n-th order diffraction lobe of the radiation pattern can be estimated using electromagnetic waves theory. Electric field vectors and propagation process of diffracted electromagnetic wave in biconical antenna are schematically demonstrated in Fig. 6. For convenience of analysis and illustration all dielectric parts are excluded from the structure. Two auxiliary designations are used in the Fig. 6. Size d stands for the diameter of biconical antenna, and θ denotes elevation angle with respect to the horizontal plane.

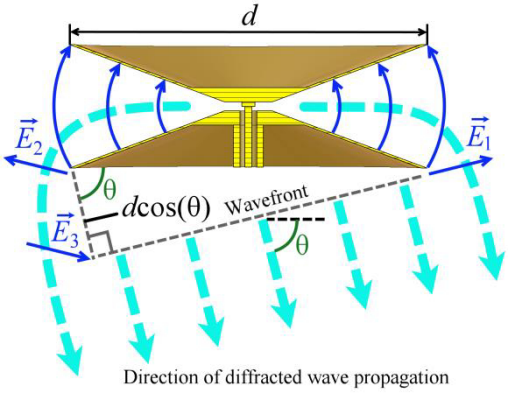

FIGURE 6. Propagation of diffracted electromagnetic wave in biconical antenna.

At any frequency, radiation of biconical antenna is absent in directions downward and upward along its symmetry axis. This is explained by mutual compensation of horizontal projections of electric field vectors from opposite parts of antenna for any azimuthal angle. For example, it is seen in Fig. 6 that horizontal components of $\vec{E}_1$ and $\vec{E}_2$ field vectors compensate each other because they have opposite directions and equal absolute values.

Another situation occurs for electromagnetic waves propagating in direction, which is inclined with respect to antenna's axis. In this case, far-field opposite electric field vectors $\vec{E}_1$ and $\vec{E}_2$ can compensate or amplify each other in transversal direction depending on type of resulting interference, which can be constructive or destructive. After reaching the position of $\vec{E}_3$ field vector, wave maintains its phase shift with respect to the wave with $\vec{E}_1$ vector because they propagate starting from the same wavefront. The kind of interference and absolute value of resulting far-field vector of electric field is determined by the additional phase shift between waves with electric fields $\vec{E}_3$ and $\vec{E}_2$, which occurs as the result of inclined propagation.

Phase shift between the phasors of electric fields $\dot{\vec{E}}_3$ and $\dot{\vec{E}}_2$ can be calculated by the following formula:

$$\Delta\varphi = \beta d\cos(\theta), \tag{1}$$

where β denotes wave number of electromagnetic waves in air. It is defined by the known expression [37]:

$$\beta = \frac{2\pi f}{c}, \tag{2}$$

where f stands for wave's frequency, and c denotes the speed of electromagnetic waves in air.

Having substituted (2) in (1), we obtain formula for the phase shift as a function of frequency f and elevation angle θ as follows:

$$\Delta\varphi = \frac{2\pi f}{c} d\cos(\theta). \tag{3}$$

As it is seen in Fig. 6, constructive interference of waves with electric fields $\vec{E}_1$ and $\vec{E}_3$ occurs in case of direction change of vector $\vec{E}_2$ to the opposite one after having passed the distance $d\cos(\theta)$. This means that vectors $\vec{E}_2$ and $\vec{E}_3$ are antiphase and phase difference (3) is as follows:

$$\Delta\varphi = (2n-1)\pi, \tag{4}$$

where n stands for a natural number.

Having performed substitution of (4) in (3), we obtain expression for determining of values of elevation angles θ_n corresponding to maximum of n-th order diffraction lobe of the radiation pattern (starting from the axial direction):

$$\theta_n = \arccos\frac{(2n-1)c}{2fd}. \tag{5}$$

Developed biconical antenna has diameter d = 120 mm and operating frequency f = 22 GHz. Using formula (5), elevation angles of maximum of 5 closest to antenna's axis diffraction lobes of radiation pattern were calculated. Besides, the elevation angles and values of these local maxima were calculated numerically using software CST Microwave Studio. Comparison of obtained theoretically and simulated results is presented in Table II.

TABLE I I. Elevation Angles and Values of Maxima of Diffraction Lobes for Antenna with 120 mm Diameter at Frequency of 22 GHz

Order of diffraction lobe (starting from biconical antenna's axis)	1	2	3	4	5
Elevation angle calculated by formula (5), °	86.7	80.2	73.5	66.6	59.2
Elevation angle calculated numerically for antenna with dielectric disc, °	85.3	77.1	70.4	63.6	56.8
Elevation angle calculated numerically for antenna without dielectric disc, °	86.1	77.3	70.3	63.7	56.8
Maximum of diffraction lobe for antenna with dielectric disc, dBi	−19.0	−18.3	−14.8	−13.9	−12.6
Maximum of diffraction lobe for antenna without dielectric disc, dBi	−9.2	−11.4	−8.8	−7.4	−5.7

It is seen from Table II that developed theoretical approach allowed calculating of elevation angles θ_1 with the accuracy of 0.6–1.4°. Elevation angles of maxima of higher order diffraction lobes are calculated with the accuracy of 3°. This can be explained by the presence of dielectric bodies in antenna structure, including dielectric disc and cylindrical spacer. They possess dielectric effect of field concentration at microwave frequencies. This results in angular shift of diffraction lobes closer to horizontal plane by 3°. On the whole, presented theoretical approach provides simple and correct physical explanation of diffraction on conical surfaces of the antenna with satisfying correlation of elevation angles corresponding to maxima of diffraction lobes.

Table II presents paramount results for values of maxima of diffraction lobes. Comparison of results for biconical antennas with and without dielectric disc shows significant reduction of diffraction lobes for the first design. Addition of dielectric disc results in lowering of the first (from axis) diffraction lobe by 10 dB compared to the antenna without disc. In the same time, each of higher order lobes is reduced by 6–7 dB.

Consequently, introduced dielectric disc is a key element of novel compact biconical antennas with protection from jamming and/or detection through diffraction lobes of radiation pattern. Similar function can be performed by a cylindrical dielectric lens of the hyperbolic profile [38], [39], but its fabrication is more complicated and more expensive in several times. Besides, mass of dielectric lens is greater compared to more compact dielectric disc, which can also be decisive factor for antenna's application on the board of a UAV.

V. MEASURED CHARACTERISTICS OF DEVELOPED BICONICAL ANTENNA WITH LOW DIFFRACTION LOBES

Structural elements of designed microwave biconical antenna were demonstrated in Fig. 2 and 3. Assembled fabricated antenna is presented in Fig. 7. Shown design contains connected waveguide-to-coaxial transition. In cross-section, applied rectangular waveguide has inner width and height equal to 11 and 5.5 mm, respectively. When antenna is applied on board of the UAV control system, rectangular waveguide port is connected directly to frequency converter.

VSWR of fabricated antenna as function of frequency was measured using microwave scalar network analyzer from rectangular waveguide port. Obtained experimental results for VSWR are illustrated in Fig. 4 by dashed line. It is seen that in frequency range 20–24 GHz measured VSWR of biconical antenna with transition is less than 1.8. At antenna's operating frequency of 22 GHz measured VSWR is equal to 1.6.

Photo of the experimental setup for measurement of designed antenna's radiation pattern in E-plane is presented in Fig. 8. As it is seen, back wall of laboratory is lined with absorbing materials to prevent reflections.

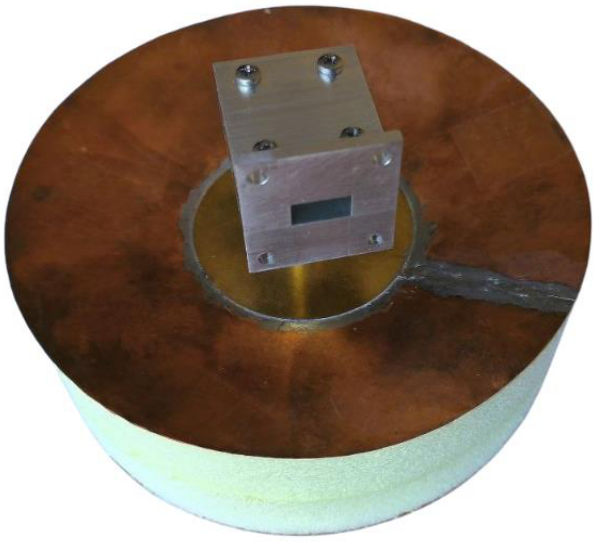

FIGURE 7. Fabricated biconical antenna with coaxial-to waveguide transition.

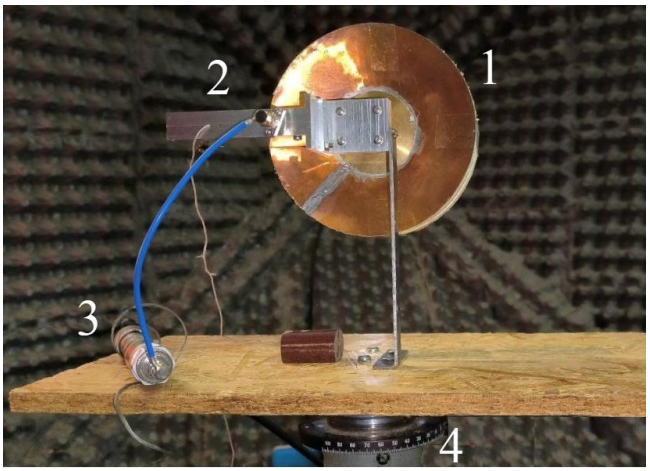

FIGURE 8. Experimental setup for measurement of E-plane radiation pattern.

Shown in Fig. 8 measurement setup includes tested biconical antenna (1), frequency converter (2), detector section (3), and accurate angular rotator (4). Using this setup we have measured E-plane radiation pattern of fabricated biconical antenna at the operating frequency of 22 GHz. Determination of biconical antenna's gain was made by comparing its received signal with signal received by a reference pyramidal horn antenna.

Obtained experimentally E-plane radiation pattern of fabricated biconical antenna is presented in Fig. 5 by dotted curve. Maximal value of measured gain is 6.3 dBi. Measured values of diffraction lobes are less than −20 dBi in range of elevation angle −30–+30° alteration from the antenna's axis (angles from −90° to −60° and from 60° to 90° in Fig. 5).

Therefore, measured characteristics of fabricated biconical antenna confirm its good matching performance and low level of diffraction lobes of radiation pattern at the operating frequency of 22 GHz.

VI. CONCLUSION

A new compact biconical antenna with low diffraction lobes of radiation pattern was developed, simulated, fabricated and tested experimentally. Theoretical analysis of diffraction phenomenon and occurrence of near-axial radiation lobes was carried out. Suggested antenna includes a dielectric disc between its conical conducting surfaces. This element provided decrement of the first (from axis) diffraction lobe by 10 dB compared to the antenna without disc. In addition, each of higher order lobes was lowered by 6–7 dB. At the operating frequency of 22 GHz fabricated antenna provides VSWR equal to 1.6 and maximal value of gain equal to 6.3 dBi. Measured diffraction lobes of radiation pattern in range of elevation angle −30–+30° from the antenna's axis are less than −20 dBi. Developed compact biconical antennas were successfully applied in modern UAV control systems with protection from jamming.

REFERENCES

[1] S. Arianos, G. Dassano, F. Vipiana, and M. Orefice, "Design of multi-frequency compact antennas for automotive communications," *IEEE Transactions on Antennas and Propagation*, vol. 60, no. 12, pp. 5604–5612, December 2012, doi: 10.1109/TAP.2012.2213052.

[2] M. Nosrati, A. Jafargholi, R. Pazoki, and N. Tavassolian, "Broadband slotted blade dipole antenna for airborne UAV applications," *IEEE Transactions on Antennas and Propagation*, vol. 66, no. 8, pp. 3857–3864, August 2018, doi: 10.1109/TAP.2018.2835524.

[3] C. Ni, J. Jiang, W.-J. Wu, L. Zhao, and Z. Fan, "Decoupling method based on complementary split ring resonator (CSRR) for two cone shipborne antennas," *IEEE Access*, vol. 9, pp. 167845–167854, 2021, doi: 10.1109/ACCESS.2021.3135577.

[4] Y. Wang, P. Bai, X. Liang, W. Wang, J. Zhang, and Q. Fu, "Reconnaissance mission conducted by UAV swarms based on distributed PSO path planning algorithms," *IEEE Access*, vol. 7, pp. 105086–105099, 2019, doi: 10.1109/ACCESS.2019.2932008.

[5] H. Huang and A. V. Savkin, "Aerial surveillance in cities: when UAVs take public transportation vehicles," *IEEE Transactions on Automation Science and Engineering*, vol. 20, no. 2, pp. 1069–1080, April 2023, doi: 10.1109/TASE.2022.3182057.

[6] H. Xu et al., "A survey on UAV applications in smart city management: challenges, advances, and opportunities," *IEEE Journal of Selected Topics in Applied Earth Observations and Remote Sensing*, vol. 16, pp. 8982–9010, 2023, doi: 10.1109/JSTARS.2023.3317500.

[7] S. K. Phang, T. H. A. Chiang, A. Happonen, and M. M. L. Chang, "From satellite to UAV-based remote sensing: a review on precision agriculture," *IEEE Access*, vol. 11, pp. 127057–127076, 2023, doi: 10.1109/ACCESS.2023.3330886.

[8] M. Aljohani, R. Mukkamala, and S. Olariu, "Autonomous strike UAVs in support of homeland security missions: challenges and preliminary solutions," *IEEE Access*, vol. 12, pp. 90979–90996, 2024, doi: 10.1109/ACCESS.2024.3420235.

[9] A. Salari and D. Erricolo, "Unmanned aerial vehicles for high-frequency measurements: an accurate, fast, and cost-effective technology", *IEEE Antennas and Propagation Magazine*, vol. 64, no. 1, pp. 39–49, February 2022, doi: 10.1109/MAP.2021.3061026.

[10] M. Erdelj, E. Natalizio, K. R. Chowdhury, and I. F. Akyildiz, "Help from the sky: leveraging UAVs for disaster management," *IEEE Pervasive Computing*, vol. 16, no. 1, pp. 24–32, Jan.-Mar. 2017, doi: 10.1109/MPRV.2017.11.

[11] H. So, "Migratory unmanned aerial vehicle system (MiUAV) for automated infrastructure inspection," *IEEE Access*, vol. 11, pp. 56392–56399, 2023, doi: 10.1109/ACCESS.2023.3282995.

[12] J. Yi, H. Zhang, S. Li, O. Feng, G. Zhong, and H. Liu, "Logistics UAV air route network capacity evaluation method based on traffic flow allocation," *IEEE Access*, vol. 11, pp. 63701–63713, 2023, doi: 10.1109/ACCESS.2023.3238464.

[13] Y. Qin, M. A. Kishk, and M.-S. Alouini, "Stochastic geometry-based trajectory design for multi-purpose UAVs: package and data delivery," *IEEE Transactions on Vehicular Technology*, vol. 73, no. 3, pp. 4136–4150, March 2024, doi: 10.1109/TVT.2023.3323682.

[14] Z. Xiaoning, "Analysis of military application of UAV swarm technology," in Proc 2020 3rd Int. Conf. on Unmanned Systems (ICUS), Harbin, China, November 2020, pp. 1200–1204, doi: 10.1109/ICUS50048.2020.9274974.

[15] Y. Cui, P. Luo, Q. Gong, and R. Li, "A compact tri-band horizontally polarized omnidirectional antenna for UAV applications," *IEEE Antennas and Wireless Propagation Letters*, vol. 18, no. 4, pp. 601–605, April 2019, doi: 10.1109/LAWP.2019.2897380.

[16] L. Scorrano et al., "Experimental investigations of a novel lightweight blade antenna for UAV applications", *IEEE Antennas and Propagation Magazine*, vol. 59, no. 2, pp. 108–178, April 2017, doi: 10.1109/MAP.2017.2655533.

[17] K. Ye, Y. Lu, Q. You, K. Wang, J. Xu, and J. Huang, "Compact dual-band shared-aperture omnidirectional biconical antenna for microwave and millimeter-wave applications," *IEEE Transactions on Antennas and Propagation*, vol. 72, no. 5, pp. 4594–4599, May 2024, doi: 10.1109/TAP.2024.3378389.

[18] S. Z. Sapuan, F. H. Herie, and M. Z. Mohd Jenu, "A new small sized wideband biconical antenna for electromagnetic compatibility (EMC) measurements", in *Proc. 2016 IEEE Asia-Pacific Conference on Applied Electromagnetics (APACE)*, Langkawi, Malaysia, December 2016, pp. 222–225, doi: 10.1109/APACE.2016.7915891.

[19] S. S. Zhekov, A. Tatomirescu, and G. F. Pedersen, "Modified biconical antenna for ultrawideband applications", in *Proc. 10th European Conference on Antennas and Propagation (EuCAP)*, Davos, Switzerland, April 2016, pp. 1–5, doi: 10.1109/EuCAP.2016.7481364.

[20] F. F. Dubrovka, S. Piltyay, M. Movchan, and I. Zakharchuk, "Ultrawideband compact lightweight biconical antenna with capability of various polarizations reception for modern UAV applications," *IEEE Transactions on Antennas and Propagation*, vol. 71, no. 4, pp. 2922–2929, April 2023, doi: 10.1109/TAP.2023.3247145.

[21] A. Dastranj and B. Abbasi-Arand, "High-performance 45° slant-polarized omnidirectional antenna for 2–66 GHz UWB applications," *IEEE Transactions on Antennas and Propagation*, vol 64, no. 2, pp. 815–820. February 2016, doi: 10.1109/TAP.2015.2509010.

[22] O. Manoochehri et al., "A dual-polarized biconical antenna for direction finding applications from 2 to 18 GHz," *Microw. Opt. Technol. Lett.* vol. 60, no. 6, pp. 1552–1558. June 2018, doi: 10.1002/mop.31195.

[23] A. Bulashenko et al., "Synthesis of waveguide diaphragm polarizers using wave matrix approach," in *Proc. IEEE 3rd Ukraine Conference on Electrical and Computer Engineering (UKRCON)*, Lviv, Ukraine, August 2021, pp. 111–116. doi: 10.1109/UKRCON53503.2021.9575322.

[24] A. V. Bulashenko, S. I. Piltyay, and I. V. Demchenko, "Wave matrix technique for waveguide iris polarizers simulation. Numerical results," *Journal of Nano- and Electronic Physics*, vol. 13, no. 5, pp. 05023-1–05023-6, October 2021. doi: 10.21272/jnep.13(5).05023.

[25] I. Fesyuk et al., "Waveguide polarizer for radar systems of 2 cm wavelength range," in *Proc. IEEE 3rd Ukraine Conference on Electrical and Computer Engineering (UKRCON)*, Lviv, Ukraine,

August 2021, pp. 15–20. doi: 10.1109/UKRCON53503.2021.9575278.

[26] A. Polishchuk et al., "Compact posts-based waveguide polarizer for satellite communications and radar systems," in *Proc. IEEE 3rd Ukraine Conference on Electrical and Computer Engineering (UKRCON)*, Lviv, Ukraine, August 2021, pp. 78–83. doi: 10.1109/UKRCON53503.2021.9575462.

[27] S. Piltyay et al., "Electromagnetic simulation of new tunable guide polarizers with diaphragms and pins," *Advanced Electromagnetics*, vol. 10, no. 3, pp. 24–30, 2021. doi: 10.7716/aem.v10i3.1737.

[28] V. Shuliak et al., "Modern microwave polarizers and their electromagnetic characteristics," in *Proc. IEEE 3rd Ukraine Conference on Electrical and Computer Engineering (UKRCON)*, Lviv, Ukraine, August 2021, pp. 21–26, doi: 10.1109/UKRCON53503.2021.9575879.

[29] A. Chakraborty, S. Dey, S. Chakraborty, and B. Gupta, "Modified clover arranged reactively loaded dual band polarization agile omnidirectional wire antenna," in Proc. 2020 URSI Regional Conference on Radio Science (URSI-RCRS), Varanasi, India, 2020, pp. 1–4, doi: 10.23919/URSIRCRS49211.2020.9113632.

[30] B. Kaswarra, W. Quddus, F. Scire Scappuzzo, and S. N. Makarov, "Circular polarization bandwidth for a bowtie turnstile over a ground plane," in Proc. 2007 IEEE Antennas and Propag. Society Int. Symp., Honolulu, USA, 2007, pp. 3544–3547, doi: 10.1109/APS.2007.4396303.

[31] S. N. Makarov, F. Scire Scappuzzo, B. Kaswarra, and W. Quddus, "Circular polarization bandwidth of a planar turnstile antenna," in Proc. *2007 IEEE Antennas and Propagation Society International Symposium*, Honolulu, USA, 2007, pp. 2646–2649, doi: 10.1109/APS.2007.4396078.

[32] O. Myronchuk, O. Shpylka, S. Zhuk, and Y. Myronchuk, "Two-stage methods for channel frequency response estimation in OFDM communication systems based on pilots from current received symbol," in *Proc. 2022 IEEE 41st International Conference on Electronics and Nanotechnology (ELNANO)*, Kyiv, Ukraine, 2022, pp. 500–505, doi: 10.1109/ELNANO54667.2022.9927031.

[33] O. Myronchuk, O. Shpylka, D. Strukov, and A. Petrovskyi, "Neural network for channel frequency response estimation in OFDM communication systems," in *Proc. 2022 IEEE 9th Int. Conf. on Problems of Infocommunications, Science and Technology (PIC S&T)*, Kharkiv, Ukraine, 2022, pp. 54–58, doi: 10.1109/PICST57299.2022.10238631.

[34] P. Li, C. Fan, S. Mesnager, Y. Yang, and Z. Zhou, "Constructions of optimal uniform wide-gap frequency-hopping sequences," *IEEE Transactions on Information Theory*, vol. 68, no. 1, pp. 692–700, Jan. 2022, doi: 10.1109/TIT.2021.3123395.

[35] A. Aleem et al., "Broad-band dielectric properties of Teflon, Bakelite, and air: Simulation and experimental study," *Materials Science and Engineering: B*, vol. 272, 115347, October 2021, doi: 10.1109/TIT.2021.3123395.

[36] X. Liang et al., "Investigations on the basic electrical properties of Polyurethane foam material," in *Proc. 2015 IEEE 11th International Conference on the Properties and Applications of Dielectric Materials (ICPADM)*, Sydney, NSW, Australia, 2015, pp. 863–866, doi: 10.1109/ICPADM.2015.7295409.

[37] D. M. Pozar, *Microwave Engineering*. Hoboken, New Jersey: John Wiley & Sons, 2012.

[38] A. M. Bobreshov et al., "Biconical antenna with inhomogeneous dielectric lens for UWB applications", *Electronic Letters*, vol. 56, no. 17, pp. 857–859, August 2020, doi: 10.1049/el.2020.1098.

[39] F. F. Dubrovka and S. I. Piltyay, "Ultrawideband microwave biconical high-gain antenna for dual-band systems of omnidirectional radio monitoring", *Radioelectronics and Communications Systems*, vol. 63, no. 12, pp. 619–632, Dec. 2020, doi: 10.3103/S0735272720120018.